DOI: 10.19884/j.1672-5220.202403021

A Compact Millimeter Wave Antenna Array with Defected Ground Structure for 5G Applications

SHAKEEL Awais[1], HAN Fang[1*], ZAHOOR Sahar[2], KHALEEQ Danish[3]
1. College of Information Science and Technology, Donghua University, Shanghai 201620, China
2. Bahauddin Zakariya University, Multan 60800, Pakistan
3. Allama Iqbal Open University, Islamabad 44310, Pakistan

Abstract: The transition towards the fifth generation (5G) of communication systems has been fueled by the need for compact, high-speed and wide-bandwidth systems. These advancements necessitate the development of novel and highly efficient antenna designs characterized by the compact size. In this paper, a novel antenna design with a hexagonal-shaped resonating element and two U-shaped open-ended stubs is presented. Millimeter-wave (mmWave) frequency range suffers from attenuation due to atmosphere and path loss because of higher frequencies. To address these issues, the deployment of a high-gain antenna is imperative. This design is created through an evolutionary process to work best in the mmWave frequency range with a high gain. A thin Rogers RT5880 substrate with a thickness of 0.254 mm, a dielectric constant of 2.3 and a loss tangent of 0.000 9 supports the copper-based radiating element. A partial ground plane with a square slot and trimmed corners at the bottom enhances the antenna's bandwidth. The single-element antenna exhibits a wide bandwidth of nearly 6 GHz and a gain of 4.58 dBi. By employing the proposed antenna array, the antenna gain is significantly enhanced to 14.90 dBi while maintaining an ultra-compact size of 24 mm × 46 mm at the resonant frequency of 31 GHz. The antenna demonstrates a wider impedance bandwidth of 15.73% (28 – 34 GHz) and an efficiency of 94%. The proposed design works well for 5G communication and satellite communication, because it has a simple planar structure and focused dual-beam radiation patterns from a simple feeding network.

Key words: dual beam; ultra-compact antenna array; millimeter wave (mmWave); 5G; high gain
CLC number: TN82 **Document code**: A
Article ID: 1672-5220(2024)05-0557-12

Open Science Identity (OSID)

0 Introduction

The fifth generation (5G) technology has become the center of attention in the worldwide telecommunication system owing to its significant potential for increased data rates, alongside the massive expansion of the system. An increase in data rates is directly associated with the improvement of the bandwidth. The millimeter-wave (mmWave) spectrum has the ability to provide 5G services with higher data rates and lower latency over the whole frequency range, according to feasibility studies[1]. The growing cellular information flow from activities like movie streaming, using social media sites and operating data centers has exceeded the capability of the fourth generation (4G) infrastructure[2-3]. As a result, in anticipation of future needs for high-speed wireless connectivity, governments throughout the globe are switching to the 5G technology.

The heightened interest in the 5G infrastructure stems primarily from the exponential surge in mobile device usage, necessitating faster data rates and wider bandwidths to cover more frequency ranges[4]. Additionally, contemporary communication infrastructure grapples with challenges such as congestion, inadequate bandwidth and restricted channel capacity within established communication networks. The mmWave wireless communication technology can support more users due to its lower latency, more channel capacity and higher data rates[5]. This allows for the smooth management of the growing number of mobile terminals used by users. The 5G spectra are split into two parts: sub-6 GHz which includes frequencies below 6 GHz, and mmWave. The allocation of the mmWave frequency spectrum for 5G, spanning from 24 GHz to 80 GHz, has been carried out by the International Telecommunication Union (ITU). Leveraging the mmWave frequency spectrum has various benefits, including increased bandwidths, multi-gigabit data transmission possibilities and the possibility of smaller antenna sizes owing to shorter wavelengths. Given the requirement for high data rates and low latency, substantial innovations are taking place in the mmWave frequency spectrum, which is presently underutilized compared to the sub-6 GHz frequency range.

Received date: 2024-03-04
Foundation item: National Natural Science Foundation of China (No. 12272092)
* Correspondence should be addressed to HAN Fang, email: yadiahan@dhu.edu.cn
Citation: SHAKEEL A, HAN F, ZAHOOR S, et al. A compact millimeter wave antenna array with defected ground structure for 5G applications [J]. *Journal of Donghua University (English Edition)*, 2024, 41(5): 557-568.

The mmWave frequency spectrum exhibits a naturally decreasing wavelength, and highlights the substantial impact of atmospheric changes[5-6]. In order to address difficulties caused by atmospheric factors, it is recommended to use mmWave frequency range antennas that have concentrated radiation patterns and exhibit higher values of the peak gain[7]. Signals in lower frequency bands may easily travel long distances and penetrate thick vegetation and towering buildings, whereas signals in higher frequency bands have shorter ranges and have a harder time piercing dense materials, so they cover less ground[8]. Due to the significant route loss encountered during propagation, mmWave technology is mostly suitable for a shorter range of distance for sake of communication. Addressing these challenges is critical for optimizing the utilization of high-frequency waves in 5G and future wireless communication systems. This necessitates the deployment of antenna arrays which exhibits higher gains not only for the transmitting station end but also for the receiving station end.

Here is the outline of the article. Section 1 explains the literature review. Section 2 elucidates the process of designing, the parametric study and the antenna array construction. Section 3 outlines the results. Section 4 provides the concluding remarks.

1 Literature Review

In recent times, 5G antennas designed for the mmWave frequency spectrum have garnered considerable attention among researchers, leading to the proposal of various antenna designs[9-10]. Planar arrays and substrate integrated waveguide (SIW) based feeding arrays are addressed to exhibit the comparison of these array types. The usefulness of SIW based devices[9] is limited to the added complexity caused by metallic vias, making them unsuitable for real-time applications in mmWave communication systems. In addition, researchers have created multilayered antennas with array topologies that are based on cavities. These antennas have a maximum gain of 13.97 dBi and can operate within a frequency range of 2.3 GHz. However, their dimensions (70 mm × 63.5 mm) are impractically large for mmWave wireless applications[11]. In contrast, a basic phased array fed with series feeding technique for patches specifically developed for 28 GHz mmWave applications presents a smaller footprint with a commendable gain; nevertheless, its narrow operating band proves inadequate for fulfilling the requirements of 5G applications[12].

For 28 GHz mmWave applications, a four-port antenna arrangement with conical rings was presented in Ref. [13]. Despite the antenna component impressive isolation which allows for pattern variety, the claimed overall gain of the multiple input multiple output (MIMO) system is 12 dBi, and the system has more than 34% impedance bandwidth and a size dimension of 45 mm × 20 mm. Nevertheless, the design is constrained by its massive dimensions and intricate framework. A microstrip antenna array with minimal cross-polarization was optimized for mmWave wireless applications, with a dimension of 56 mm × 14 mm × 2 mm and a gain of 14.5 dBi[14]. The limited applicability of the array is due to its multi-layered architecture with two printed circuit board (PCB) layers for the coupling feed structure. Furthermore, in a separate research, an array of MIMO antennas was suggested[15]. The array would function in the 37 GHz frequency region, which is reserved for mmWave 5G communication system. The gain of the antenna may increase from 6.84 dBi per element to 12.80 dBi when an array of four elements is used.

A small patch antenna array with a wide bandwidth was created to operate at 60 GHz[16]. By using an asymmetric feeding method, power is distributed unevenly throughout the components of a 1 × 8 array, leading to a gain fluctuation between 12 dBi and 16 dBi. To reduce radiation emission in the opposite direction and maintain a single beam, a complete ground plane is used together with an electromagnetic band-gap (EBG) reflector placed below the array structure. The EBG structure allows achieving a 14 dBi gain with a high efficiency at 58 GHz. Yet, the design becomes bulky because of several layers, which is its only downside. A new 1 × 8 antenna array designed for mmWave applications with reduced cross-polarization was proposed in Ref. [17]. Planar antenna arrays are easier to manufacture than SIWs. Transmission line losses are higher than SIW losses, but they may be ignored by meticulous feed network planning.

There are systems based on SIWs, but they are complicated and hard to integrate. It is necessary to find a way to make them simpler and easier to construct. An easy way to increase the gain is by using an array method which involves arranging many antenna elements in a certain arrangement. For 5G networks that use the mmWave frequency spectrum which includes the 31 GHz frequency, there is a big need for small array designs that have a high gain, a broad impedance bandwidth and a small footprint. 5G networks and satellite communication may both benefit from an antenna that is built to operate at 31 GHz[18]. Because of its smaller size, less weight and conformity with standards, this article suggests an eight-element linear patch array that operates at 31 GHz.

2 Antenna Design and Construction

2.1 Single microstrip patch antenna design

The single-element antenna was designed and simulated utilizing ultra-thin Rogers RT5880 with a thickness of 0.254 mm, a dielectric constant of 2.3 and a loss tangent of 0.000 9. Using dielectric materials with lower loss tangents and smaller dielectric constants would effectively reduce the patch dielectric radiation and overall total losses, regardless of the characteristic impedance, compared to the materials with higher dielectric constants

and thicker substrates. To achieve resonance within the necessary frequency range, a hexagonal frame is placed at one end of the feed line, including three stubs arranged in a U shape to produce resonators. These stubs help the antenna resonate at the desired frequency. The suggested antenna consists of a defective ground plane with a tiny square notch in the top center to expand the bandwidth and round corners at the top to increase the realized gain. The antenna is activated by a microstrip line. The single antenna hexagonal patch is built using equations determining the radius of the circle, resulting in exact geometric dimensions that are favorable to the desired performance characteristics:

$$a = \frac{F}{\sqrt{1 + \frac{2h}{\pi\varepsilon_r F}\left[\ln\left(\frac{\pi F}{2h}\right) + 1.722\,6\right]}}, \tag{1}$$

$$F = \frac{8.791 \times 10^9}{f_r\sqrt{\varepsilon_r}}, \tag{2}$$

where f_r is the resonance frequency or the operating frequency; a is the patch radius; h is the substrate height; ε_r is the relative permittivity of the dielectric substrate. Length L_g and width W_g of the ground can be found by:

$$L_g = 6h + a, \tag{3}$$

$$W_g = 6h + a. \tag{4}$$

In Fig. 1(a), x_a denotes the width of the ground, y_a denotes the length of the ground, d_y represents the length of the feedline, r_1 signifies the radius of the hexagonal structure, m_1 corresponds to the length of the vertical stub, m_2 denotes the length of the horizontal stub, and u_1 represents the length of the two open-ended U-shaped stubs. Similarly, in Fig. 1(b), c_a represents the length of the defected ground structure, c_c denotes the value of the corner trimmed, while d_{sx} and d_{sy} signify the width and the depth of the ground square slot, respectively.

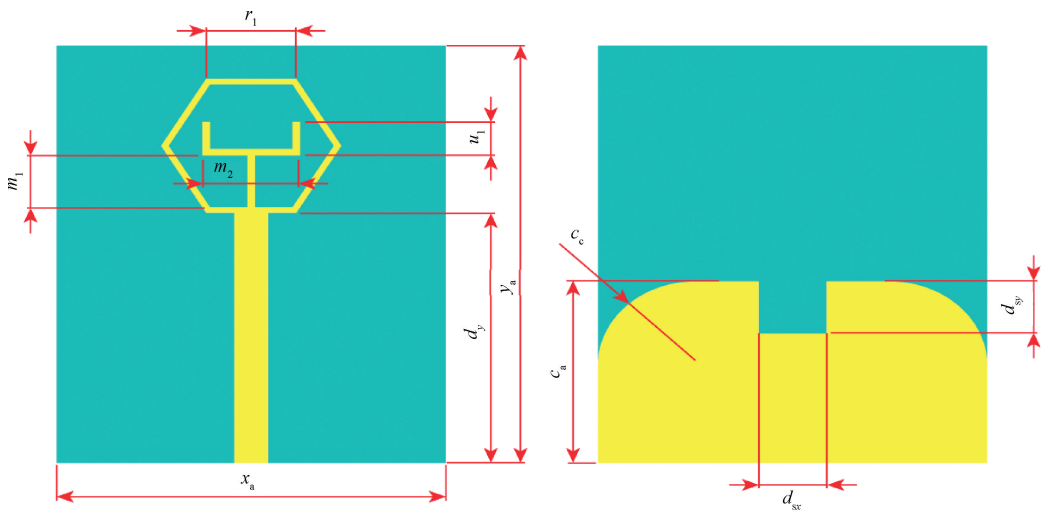

Fig. 1 Single-element antenna design with variables: (a) front view; (b) back view

Notably, the inclusion of the trimmed corner c_c contributes to an enhancement in the realized gain of the proposed antenna. The proposed antenna is refined via four evolutionary phases, as seen in Fig. 2. In the first step, a very narrow feedline in the vertical direction is introduced, resulting in poor impedance matching and the lack of a specified resonance frequency. In the second step, a circular-shaped patch is applied above the strip line, which improves impedance matching but does not attain appropriate resonance. In the third step, a stub in the horizontal direction is introduced at the top of the feed line, as well as a U-shaped resonator made from three stubs. This step improves impedance matching, resulting in resonance at the target frequency, although with poor return loss and realized gain. In the fourth stage, a hexagonal patch substitutes the circular patch, allowing for the necessary resonance frequency and the acceptable realized gain. At this point, resonance occurs at 31 GHz. The evolutionary phase demonstrates that reducing the participation of metallic components at high frequencies improves the efficiency and maximize the desired higher value of the gain within the working bandwidth. The design has been optimized to possess a length of 10 mm and a width of 8 mm with a conductive material thickness t of 0.018 mm. The detailed measurements are provided in Table 1.

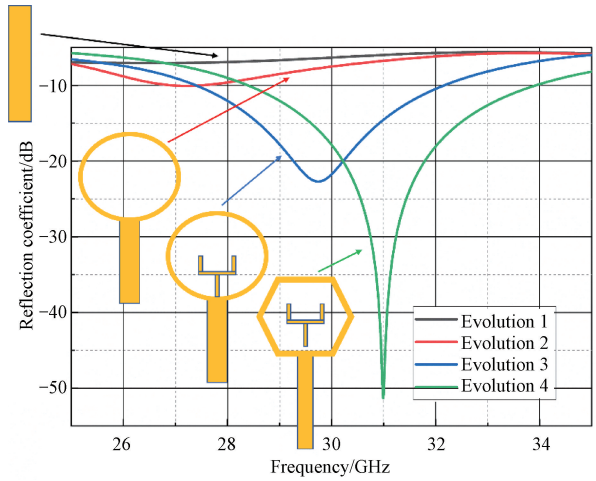

Fig. 2 Step by step design evolution

Table 1 Dimensions of proposed antenna (unit: mm)

Variable	x_a	h_1	d_{sy}	m_1	u_1	c_c	t
Value	8	0.254	1.2	1.1	0.65	2	0.018
Variable	y_a	d_{sx}	d_y	m_2	r_1	c_a	
Value	10	1.4	6	2	1.85	4.35	

The flow chart illustrating the design process of the proposed antenna is presented in Fig. 3. The substrate material Rogers RT5880 is chosen due to its low dielectric constant value. The subsequent steps involve selecting the shape of the patch, starting from circular and progressing to the final hexagonal shape with a U-shaped stub inside, alongside a square slot defected ground structure. Optimization of the square slot in the ground and other antenna parameters is carefully carried out to attain the desired performance for the single element. Then arrays of two, four and ultimately eight elements are designed to achieve a higher gain, with careful adjustment of array parameters.

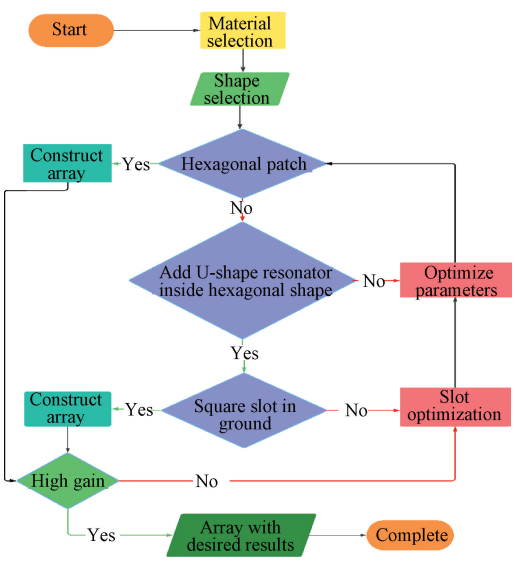

Fig. 3 Comprehensive depiction of sequential steps in designing

2.2 Parametric study

The proposed antenna was analyzed through a series of simulations, focusing primarily on the open-ended U-shaped stub within the hexagonal design and also by changing the length and the width of the slot introduced in the ground plane. The length of the U-shaped stub played a crucial role in achieving impedance matching along the hexagonal frame, as illustrated in Fig. 1. The feedline length was intentionally set above 5 mm to facilitate attachment of a radio-frequency SMA (Subminiature version A) connector, as a compact feedline would adversely impact resonance when it was in close proximity to the connector. It is observed that decreasing the length of the ground plane results in an increased bandwidth but significantly reduces the gain. Conversely, increasing the length of the ground leads to a decrease in the bandwidth proportional to the gain increase. This gain enhancement is attributed to the reduction of the back-lobe beam and the simultaneous rise in the front beam, facilitated by the utilization of a full ground plane to create a directional pattern.

In the far field, small side lobes are observed due to the impact of surface waves. A parametric study involving varying lengths of the feed and the ground plane reveals that the matching of the reflection coefficient S_{11} peak decreases as the length of the feed decreases. Additionally, a square slot is incorporated at the middle section just below the feed to broaden the operating bandwidth. Dimensions are selected based on the parametric study, ensuring that S_{11} remains above −45 dB, indicating good impedance matching. Moreover, optimization of the square slot at the top of

the partial ground plane enhances the overall performance of the design, as this slot plays a crucial role in tuning the resonance response.

When the radius of the hexagonal frame rises, the resonance frequency shifts towards the lower frequency band, and vice versa as demonstrated in Fig. 4(a). r_1 is crucial in adjusting the resonance to the specific frequency of 31 GHz. As the frequency increases, the decibel value of the reflection coefficient falls, indicating an impedance mismatch. Upon analyzing the data, the ultimate value of r_1 is selected. d_y is selected to be 6.0 mm in order to achieve a matching reflection coefficient, as shown in Fig. 4(b).

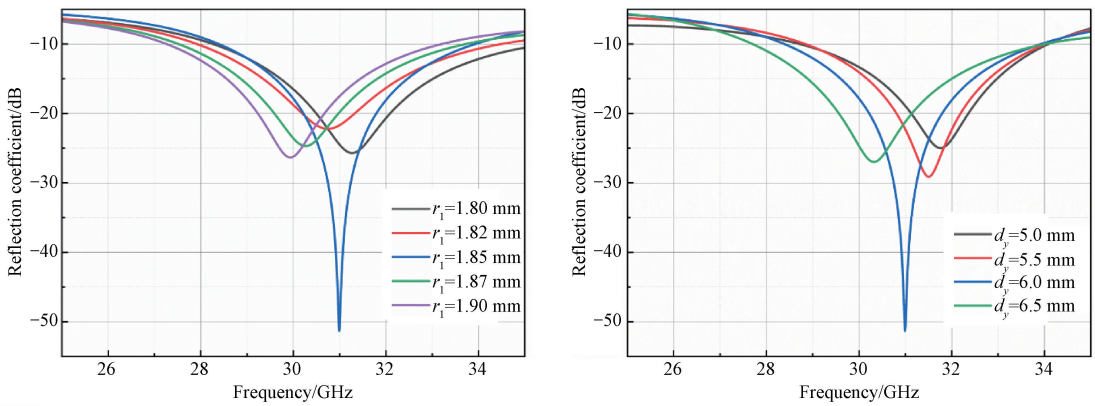

(a) (b)

Fig. 4 Reflection coefficient parametric study with respect to (a) r_1; (b) d_y

As shown in Fig. 5(a), d_{sx} is examined in order to match it with the correct resonant band. The operational band grows until it reaches a certain threshold as d_{sx} increases. When the circuit size drops below this point, the resonating band moves down within the frequency range. As shown in Fig. 5(b), the return loss of the antenna is affected by d_{sy}. As d_{sy} goes down, the return loss goes down as well, and the resonance response goes down in reflection coefficients at the same time.

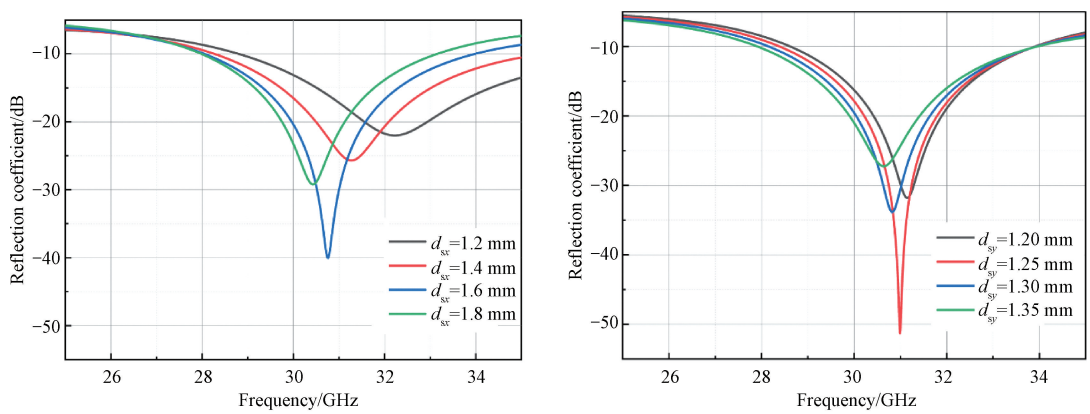

(a) (b)

Fig. 5 Reflection coefficient parametric study with respect to (a) d_{sx}; (b) d_{sy}

The parametric study on the gain of the single element with respect to d_{sx} is depicted in Fig. 6(a). d_{sx} is carefully selected to be 1.4 mm as an increase in d_{sx} results in improved gains but at the same time the value of reflection coefficient decreases and the voltage standing wave ratio (VSWR) moves farther from 1 which is an ideal value. Gain parametric study of the single element with respect to d_{sy} is depicted in Fig. 6(b). d_{sy} is considered as 1.25 mm. At this value, the proposed antenna exhibits well matched reference impedance, improved reflection coefficient parameter, better gain and increased efficiency as compared to other values of d_{sy}.

Gain parametric study with respect to the radius of the hexagonal structure is depicted in Fig. 7(a). As r_1 increases, it results in increase in the gain, but the remaining parameters deviates from the resonance frequency. d_y also affects the value of the gain as shown in Fig. 7(b). The higher value of d_y reduces the compactness of the proposed antenna.

The conductive material used is copper (annealed) with a thickness of 0.018 mm. If the thickness of the conductive material increases, the reflection coefficient and the gain parameters decrease as depicted in Fig. 8(a) and 8(b), respectively.

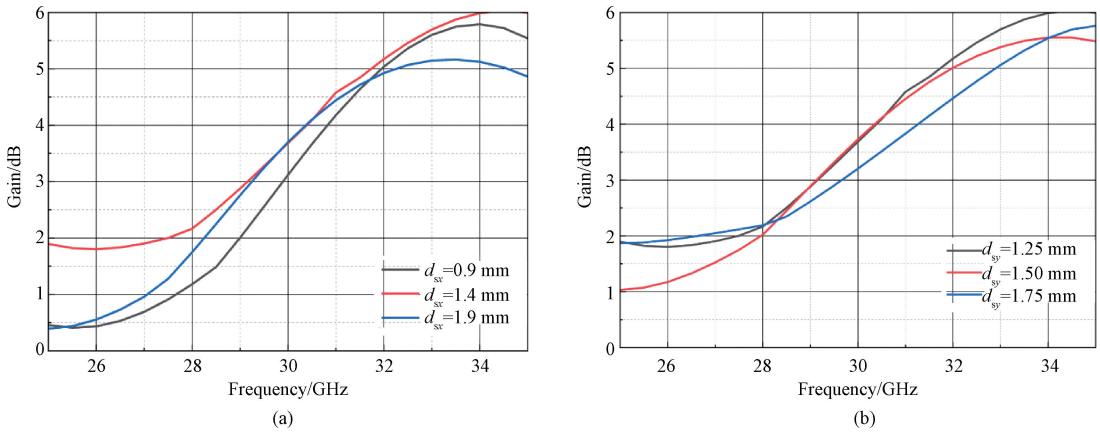

Fig. 6 Gain parametric study of single element with respect to (a) d_{sx}; (b) d_{sy}

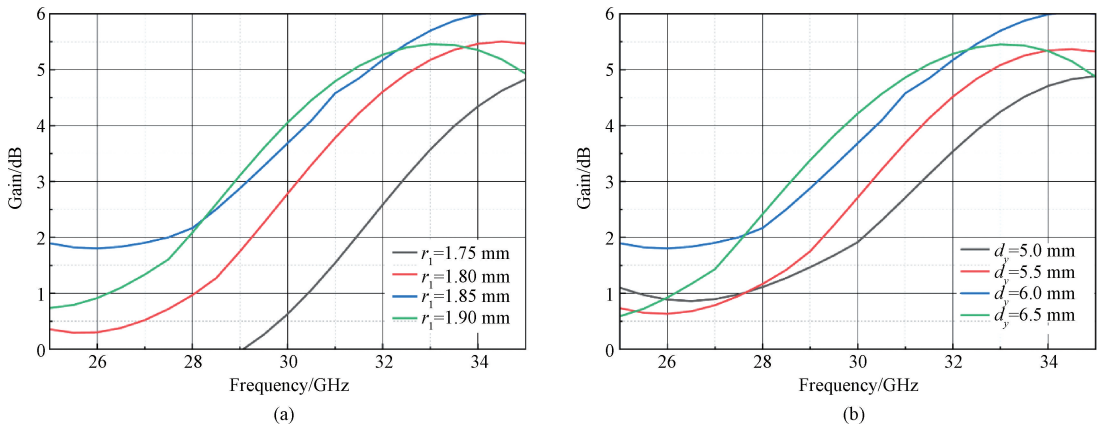

Fig. 7 Gain parametric study of single element with respect to (a) r_1; (b) d_y

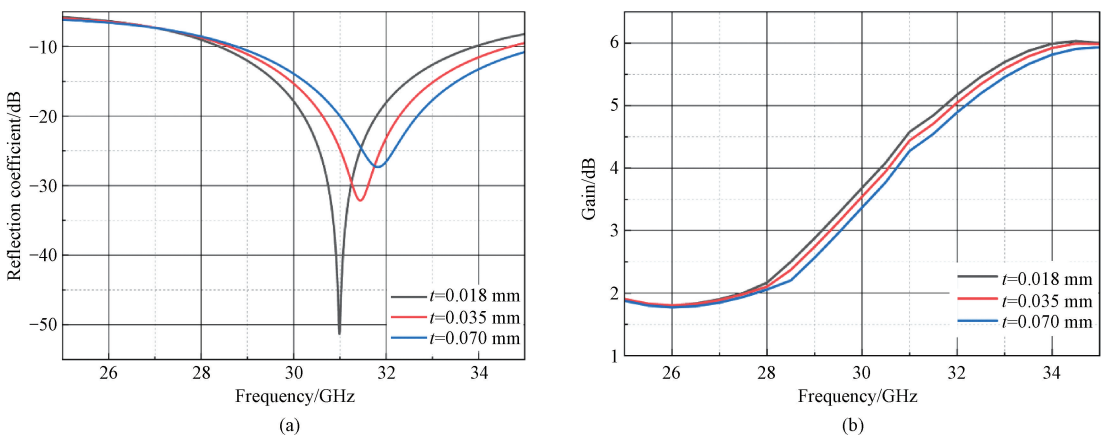

Fig. 8 Parametric study with respect to conductive material thickness: (a) reflection coefficient; (b) gain

The radiation patterns of the proposed antenna array are depicted for both the E plane and the H plane, corresponding to the azimuthal angle of the H plane at $\Phi = 90°$ and $\Phi = 0°$, respectively. In Fig. 9 (a), the E plane illustrates two nulls emitting radiation in all directions, leading to the formation of two distinct beams. Conversely, the H plane demonstrates the directivity with a beam width of 20°. Further clarity regarding the dual-beam characteristics of the proposed single-element antenna is evident in Fig. 9 (c), presenting a 3D far field plot of the proposed.

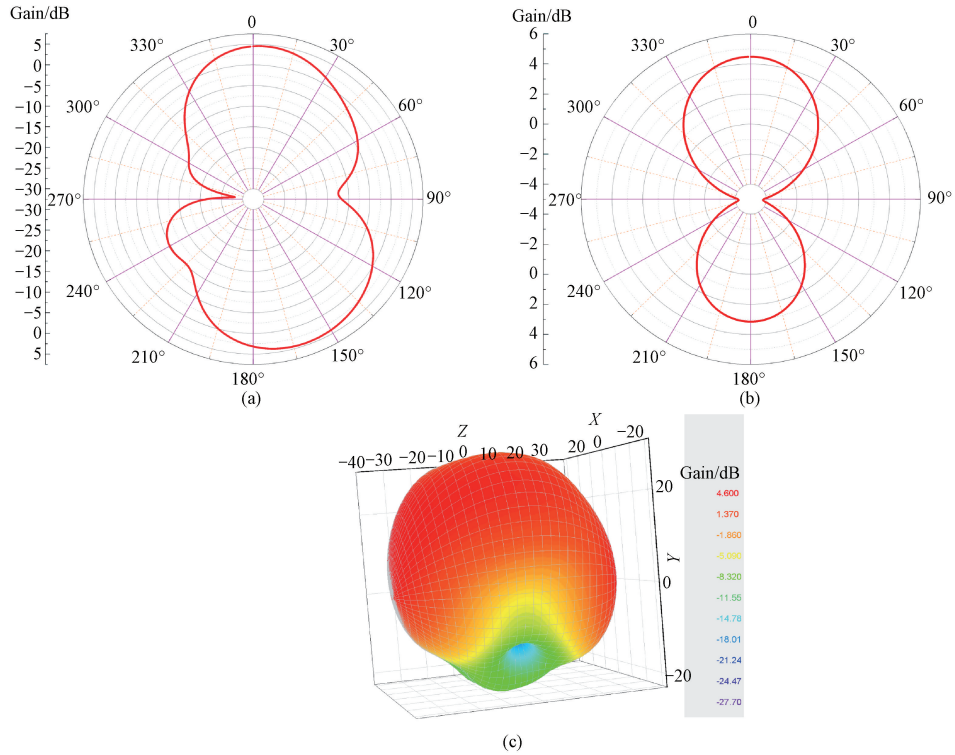

Fig. 9 Single element polar plots: (a) E-plane plot; (b) H-plane plot; (c) 3D plot

The parametric study of the U-shaped resonator is displayed in Fig. 10. m_1 is directly connected to the feedline. m_2 is introduced, together with u_1 vertical stubs placed at the corners of the horizontal stub, resulting in the creation of a U-shaped resonator. A stub not only helps in achieving acceptable return loss but also facilitates in the reduction of the hexagonal radius. Likewise, the thickness of U-shaped stab and vertical stub inside the hexagonal shape patch g_2 is selected 0.20 mm and then 0.15 mm. Through deep examination of parametric studies, the U-shaped resonator is optimized effectively, resulting in an improved realized gain.

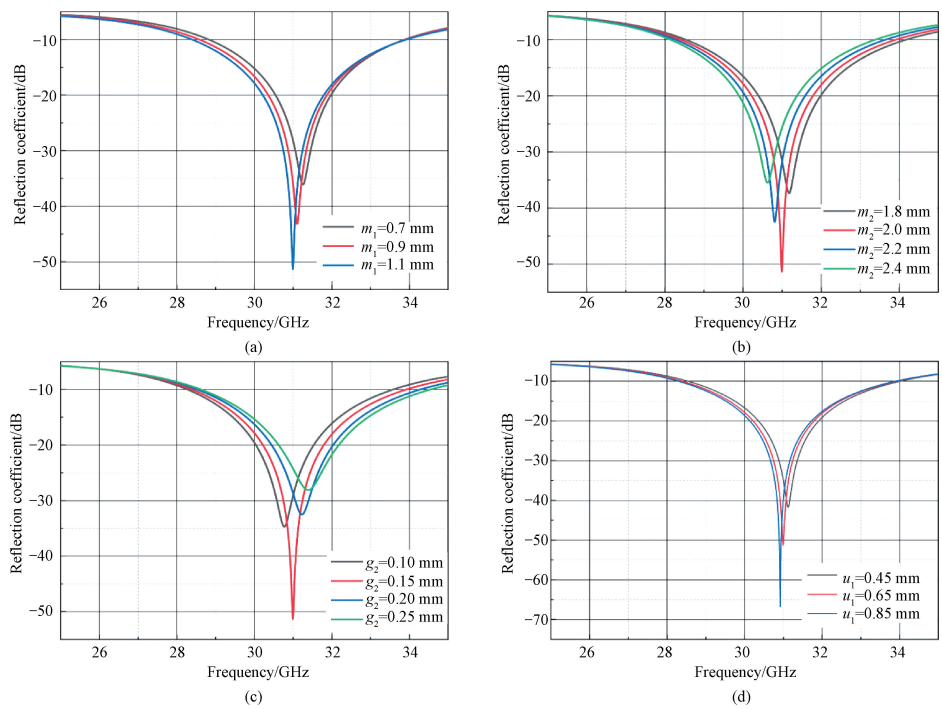

Fig. 10 S_{11} parametric study with respect to (a) m_1; (b) m_2; (c) g_2; (d) u_1

In order to be considered as a potential choice for future mmWave RF devices, an antenna must have a 50 Ω input impedance that matches with connected devices, and it should have an acceptable VSWR ranging from 1 to 2, as shown in Fig. 11. Antennas with VSWR values near to 1 are regarded to be well matched.

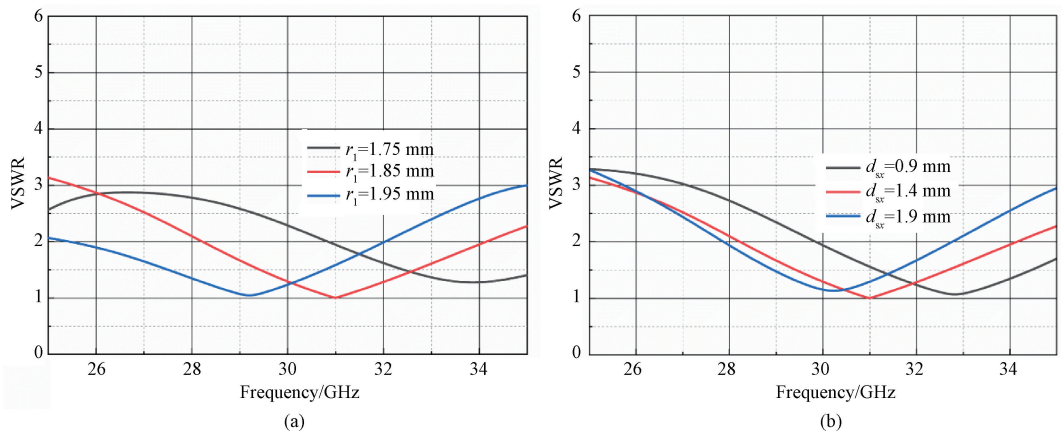

Fig. 11 VSWR parametric study with respect to (a) r_1; (b) d_{sx}

2.3 Eight-element array design

A higher value of the gain is an essential requirement of current 5G wireless communication systems to mitigate the fading effect in wireless communication and reduce the signal loss due to atmospheric attenuation. For practical 5G applications, a minimum gain of 12.0 dBi is necessary. The proposed antenna is first modified to two elements and then to a four-element linear array to meet this criterion, and then it is enlarged to an eight-element array to reach a gain higher than 14.8 dBi. The first step is to create and optimize a basic feeding network for 31 GHz. A 50 Ω feedline which is 0.9 mm wide, is split into two 100 Ω feedlines which are 0.3 mm wide each. Four 70.7 Ω feedlines, each having a thickness of 0.54 mm, are further separated from each feedline in order to feed the four design parts. The design is transformed into an eight-element antenna array by duplicating this feed network layout. Because of transmission losses, the 4.58 dBi gain that each radiator provides on its own is inadequate for real-world applications. With two elements, the power divider optimizes the gain to 8.5 dBi. With four elements, it rises to 11.7 dBi. With eight elements, it reaches 14.9 dBi. Figure 12 shows the eight-element linear planar array using a power divider with Z_1 = 50 Ω, Z_2 = 70 Ω, and Z_3 = 100 Ω as impedance matching parameters. In Fig. 12, Z_{L1}, Z_{L2} and Z_{L3} represent lengths of impedance lines, respectively; D_1, D_2 and D_3 represent the distances of the feedline between eight, four and two elements, respectively; x_1 and y_1 are the width and the length of eight elements, respectively; c_1 is the length of the defected ground structure.

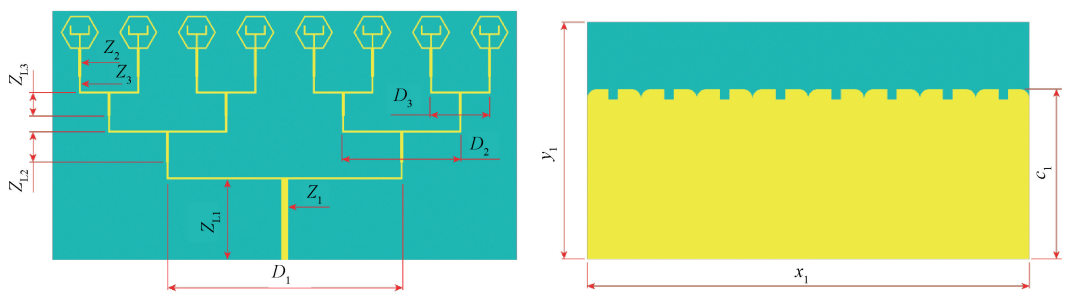

Fig. 12 Proposed design of eight-element antenna array: (a) front view; (b) back view

For mmWave antenna applications, this study presents a new and basic planar construction with a feed network that consists of an eight-element hexagonal array with U-shaped stubs. Antenna components are spaced at a constant of $\lambda/4$ apart at 31 GHz to reduce coupling. In the array structure, there is a slight reduction in the bandwidth due to the presence of a power divider. This reduction is attributed to minor losses within the array network resulting from the excitation of each antenna element. The proposed design is developed through rigorous parametric research and subsequently transformed into an array configuration. The detailed measurements of the eight-element array are given in Table 2.

Table 2 Dimensions of eight-elemant antenna array

(unit: mm)

Variable	x_1	t	Z_{L2}	D_1	D_3
Value	46	0.018	3	23.38	5.9
Variable	y_1	Z_{L1}	Z_{L3}	D_2	c_1
Value	24	8	2.25	11.7	16.7

3 Results and Discussion

With a reference level of −10 dB, the impedance bandwidth extends from 28 GHz to 34 GHz. The bandwidth that has been attained is sufficient to cover the spectrum needed for 5G mmWave applications. The proposed array has a simple feeding network and is small, hence it has low loss characteristics. At 31 GHz, the radiation pattern of the proposed design is shown in the far field. As seen in Fig. 13, there are no other major lobes present, except for the dual beams. Achieving the required radiation characteristics with little interference from undesirable lobes is an indication of how well the design works.

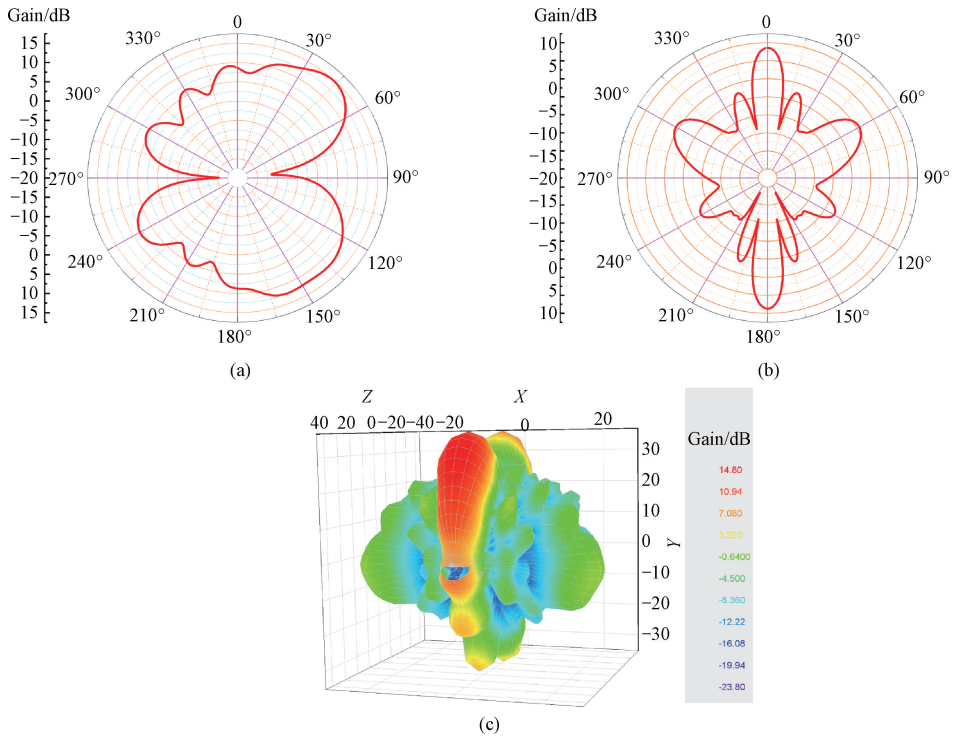

Fig. 13 Far field results: (a) E-plane plot; (b) H-plane plot; (c) 3D plot

The inherent radiation emphasizing capabilities of the array strengthens its suitability for use in satellite communication and point-to-point 5G communication systems. Its compact and flat shape makes it easy to incorporate into contemporary communication systems and gadgets. The array performance has been thoroughly tested, considering important parameters including a gain, a directivity, a radiation pattern and a return loss. To achieve a small footprint in the finished product without sacrificing performance, the power divider has been fine-tuned. Throughout the required working spectrum, the overall efficiency values stay over 90%, and the antenna efficiency response approaches more than 90% at the resonance frequency. There is a directivity of 15.2 dBi and a peak array gain of 14.9 dBi at 31 GHz.

For the eight-element feed network, the suggested approach highlights dual-beam radiation patterns with a high gain. The suggested architecture is a strong contender for 5G communication systems. For effective transmission, the narrow and directed beam widths that accompany this high gain are crucial. Also, in order to have higher data rates in the mmWave spectrum, a wider bandwidth is required. Figure 14 depicts the variation in the reflection coefficient, the radiation efficiency and the gain across different frequencies for the single-element, two-element, four-element and eight-element array configurations. These visual representations effectively demonstrate the significant enhancement in the array gain while maintaining a compact and concise size.

The evolution of the antenna array, starting from a single-element setup and expanding to an eight-element array, showcases significant improvements in important performance measures that are essential for 5G wireless communication applications and satellite communication. These improvements involve the continuous enhancement of characteristics such as the reflection coefficient, the radiation efficiency, the VSWR, the gain and the bandwidth. These improvements make the antenna array a strong contender for meeting the high requirements of 5G wireless communication systems and satellite communication networks.

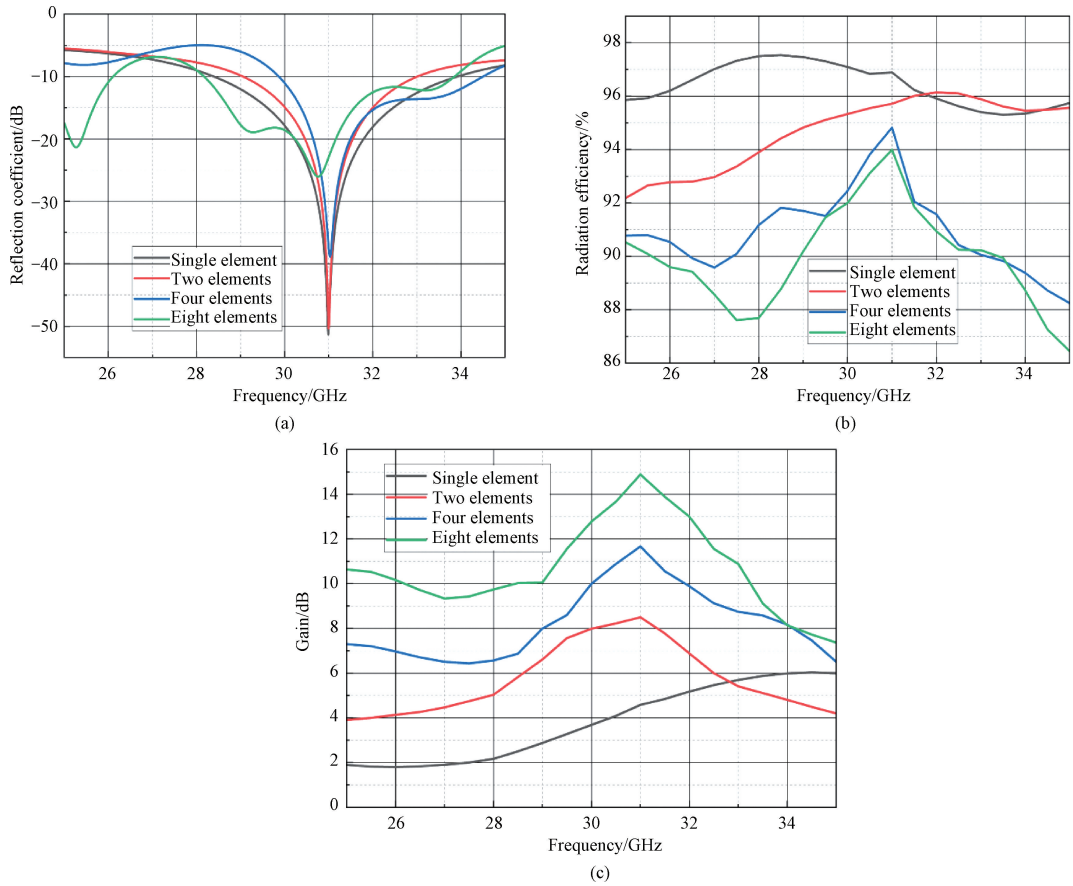

Fig. 14 All designed element result vs frequency: (a) reflection coefficient; (b) radiation efficiency; (c) gain

Planar antenna arrays are known for their narrow bandwidth responses, which makes it difficult for them to achieve a wider bandwidth. Planar structures are still the way to go since they are easier to design and fabricate than multilayer, stacked, or SIW systems. Notwithstanding these obstacles, the suggested planar antenna array shows promise in terms of performance, making it a good fit for high-tech communication networks.

A comparative analysis between the construction of an eight-element array antenna proposed in this study and the findings reported in recent literature is presented in Table 3. Unlike previous eight-element arrays in Refs. [7, 15–16] which are typically either multi-layered or based on SIW structures, the proposed antenna adopts a single-layer planar construction. While SIW-based and multi-layered antennas may exhibit favorable performance characteristics, they often entail complex architectures and larger volumes, posing challenges in manufacturing. In contrast, the proposed antenna, despite employing a basic feeding mechanism, achieves a notable gain of 14.9 dBi and a bandwidth of 6 GHz. These performance characteristics surpass those reported in the articles included in Table 3. The high gain and the wide bandwidth of the antenna render it suitable for deployment in 5G mmWave devices, highlighting its potential for advancing next-generation wireless communication systems.

Table 3 Table comparing the proposed antenna with that in existing literature

Ref.	Antenna element	Bandwidth/GHz	Configuration	Length × Width/(mm×mm)	Efficiency/%	Gain/dBi
[5]	2 × 2	3	Planar	30 × 30	90	6.1
[6]	2 × 2	2.5	Planar	30 × 30	90	7
[7]	1 × 8	2.3	SIW	63.5× 70	62	13.5
[9]	1 × 4	9	SIW	20 × 45	85	12.1
[10]	1 × 4	0.6	Planar	20 × 26	90	12.5
[14]	1 × 4	1	Planar	20 × 8	85	12.8
[15]	1 × 8	6	Multi-layer	17.5×22	94	14.2
[16]	1 × 8	10	SIW	58 × 9.3	94	14.5
Proposed	1 × 8	6	Planar	24.5×46	94	14.9

4 Conclusions

Specifically, for 5G wireless communication applications, this work introduced a small eight-element planar linear array. To attain optimum performance in the mmWave frequency spectrum, the proposed design included a unique modified structure with two open-ended U-shaped stubs and hexagonal-shaped resonating components. This structure was produced via an evolutionary approach. The proposed device had remarkable properties at 31 GHz, such as an efficiency for a single element surpassing 96%, a gain of 4.58 dBi, and a return loss of −50 dB. A high gain of 14.9 dBi was achieved by converting the proposed single-element antenna design into an eight-element linear array system using a simple feeding scheme. At the resonance frequency, the radiation pattern of the proposed design exhibited narrow E-field features, and its radiation efficiency was more than 90%. The anticipated antenna had a wider impedance bandwidth of 15.73% (28–34 GHz), a directivity of 15.1 dBi, an efficiency of 94% and a maximum realized gain of 14.9 dBi. Extensive optimizations and simulations have produced very positive results, with the eight-element linear array measuring 24 mm×46 mm, and a high gain is essential for many application situations in mmWave 5G devices. Internet of Things, mmWave and microwave sensing, 5G and autonomous vehicle applications are ideal for straightforward planar construction.

References

[1] ZHANG J, YU X H, LETAIEF K B. Hybrid beamforming for 5G and beyond millimeter-wave systems: a holistic view[J]. *IEEE Open Journal of the Communications Society*, 2020, 1: 77-91.

[2] PRZESMYCKI R, BUGAJ M, NOWOSIELSKI L. Broadband microstrip antenna for 5G wireless systems operating at 28 GHz[J]. *Electronics*, 2020, 10(1): 1.

[3] KIM G, KIM S. Design and analysis of dual polarized broadband microstrip patch antenna for 5G mmWave antenna module on FR4 substrate [J]. *IEEE Access*, 2021, 9: 64306-64316.

[4] ALMASHHDANY M B, AL-ANI O A, SABAAWI A M A, et al. Design of multi-band slotted mmWave antenna for 5G mobile applications [J]. *IOP Conference Series: Materials Science and Engineering*, 2020, 881 (1): 012150.

[5] KAMAL M M, YANG S Y, REN X C, et al. Infinity shell shaped MIMO antenna array for mm-wave 5G applications [J]. *Electronics*, 2021, 10(2): 165.

[6] RAHMAN S, REN X C, ALTAF A, et al. Nature inspired MIMO antenna system for future mmWave technologies [J]. *Micromachines*, 2020, 11(12): 1083.

[7] PARK S J, SHIN D H, PARK S O. Low side-lobe substrate-integrated-waveguide antenna array using broadband unequal feeding network for millimeter-wave handset device [J]. *IEEE Transactions on Antennas and Propagation*, 2016, 64(3): 923-932.

[8] ZHU Q, NG K B, CHAN C H, et al. Substrate-integrated-waveguide-fed array antenna covering 57–71 GHz band for 5G applications[J]. *IEEE Transactions on Antennas and Propagation*, 2017, 65(12): 6298-6306.

[9] ULLAH H, TAHIR F A. A broadband wire hexagon antenna array for future 5G communications in 28 GHz band[J]. *Microwave and Optical Technology Letters*, 2019, 61(3): 696-701.

[10] WANG N, LI M D, KUANG Y, et al. Comparison of output voltages from radio frequency energy harvesting system with textile microstrip single-element and array antennas as the receiving antennas[J]. *Journal of Donghua University (English Edition)*, 2024, 41(3): 275-281.

[11] KHAN J, ALI SEHRAI D, ALI U. Design of dual band 5G antenna array with SAR analysis for future mobile handsets [J]. *Journal of Electrical Engineering & Technology*, 2019, 14(2): 809-816.

[12] SUN G H, WONG H. A planar millimeter-wave antenna array with a pillbox-distributed network [J]. *IEEE Transactions on Antennas and Propagation*, 2020, 68(5): 3664-3672.

[13] MA Y C, WANG J H, LI Z, et al. Planar annular leaky-wave antenna array with conical beam[J]. *IEEE Transactions on Antennas and Propagation*, 2020, 68(7): 5405-5414.

[14] KHALILY M, TAFAZOLLI R, RAHMAN T A, et al. Design of phased arrays of series-fed patch antennas with reduced number of the controllers for 28-GHz m-wave applications [J]. *IEEE Antennas and Wireless Propagation Letters*, 2016, 15: 1305-1308.

[15] KHAN J, ULLAH S, ALI U, et al. Design of a millimeter-wave MIMO antenna array for 5G communication terminals[J]. *Sensors*, 2022, 22 (7): 2768.

[16] GHATTAS A S W, SAAD A A R, KHALED E E M. Compact patch antenna array for 60 GHz millimeter-wave broadband applications [J]. *Wireless Personal Communications*, 2020, 114 (4): 2821-2839.

[17] FU Y Z, LIN Y X, SHI C D. A low cross-polarization microstrip antenna array for millimeter wave applications[J]. *International Journal of Antennas and Propagation*, 2023, 2023: 7622014.

[18] KADIYAM S, JHANSI RANI A. Design and analysis of a high gain millimeter-wave antenna array for dual purpose applications[J]. *Wireless Personal Communications*, 2023, 130(1): 593-607.

适用于 5G 通信的具有缺陷接地结构的紧凑型毫米波天线阵列

SHAKEEL Awais[1], 韩　芳[1*], ZAHOOR Sahar[2], KHALEEQ Danish[3]

1. 东华大学 信息科学与技术学院, 上海 201620, 中国
2. 巴哈德因·扎卡里亚大学, 木尔坦 60800, 巴基斯坦
3. 阿拉玛·伊克巴尔开放大学, 伊斯兰堡 44310, 巴基斯坦

摘　要: 对紧凑、高速和宽带宽系统的需求, 推动了通信系统向第五代 (the fifth generation, 5G) 过渡。这些进步促使具有紧凑尺寸的新型高效天线设计的开发。该文提出了一种新型天线的设计, 该天线具有一个六边形谐振元件和两个 U 形开口短截线。毫米波频率范围会因大气层而衰减, 而由于频率较高, 路径损耗会受到影响。为了解决这些问题, 部署高增益天线势在必行。该设计是通过从单个天线到天线阵列的逐步进化过程创建的, 可在毫米波范围内以高增益工作。厚度为 0.254 mm、介电常数为 2.3、损耗角正切为 0.000 9 的薄 Rogers RT5880 基板支撑铜基辐射元件。带有方形插槽和底部修剪角的部分接地层增强了天线带宽。单晶天线具有近 6 GHz 的宽带带宽和 4.58 dBi 的增益。通过采用所提出的天线阵列, 天线增益显著提高到 14.9 dBi, 同时可在谐振频率为 31 GHz 时保持 24 mm× 46 mm 的超紧凑尺寸。该天线具有 15.73% (28~34 GHz) 的较宽阻抗带宽, 效率为 94%。所提出的设计具有简单的平面结构和来自简单馈送网络的聚焦双波束辐射模式, 适用于 5G 和卫星通信。

关键词: 双波束; 超紧凑型天线阵列; 毫米波; 5G; 高增益